

Rescuing high-scale leptogenesis using primordial black holes

Nicolás Bernal^{1,*}, Chee Sheng Fong^{2,†}, Yuber F. Perez-Gonzalez^{3,‡} and Jessica Turner^{3,§}

¹*Centro de Investigaciones, Universidad Antonio Nariño, Carrera 3 este # 47A-15, Bogotá, Colombia*

²*Centro de Ciências Naturais e Humanas Universidade Federal do ABC,
09.210-170, Santo André, SP, Brazil*

³*Institute for Particle Physics Phenomenology, Durham University,
South Road, DH1 3LE, Durham, United Kingdom*



(Received 4 April 2022; accepted 2 August 2022; published 18 August 2022)

We explore the interplay between light primordial black holes (PBH) and high-scale baryogenesis, with a particular emphasis on leptogenesis. We first review a generic baryogenesis scenario where a heavy particle, X , with mass, M_X , produced solely from PBH evaporation decays to generate a baryon asymmetry. We show that the viable parameter space is bounded from above by $M_X \lesssim 10^{17}$ GeV and increases with decreasing M_X . We demonstrate that regions of the leptogenesis parameter space, where the lightest right-handed neutrino (RHN) mass $M_{N_1} \gtrsim 10^{15}$ GeV and neutrino mass scale $m_\nu \gtrsim 0.1$ eV, excluded in standard cosmology due to $\Delta L = 2$ washout processes, become viable with the assistance of light PBHs. This scenario of PBH-assisted leptogenesis occurs because the PBHs radiate RHNs via Hawking evaporation late in the Universe's evolution when the temperature of the thermal plasma is low relative to the RHN mass. Subsequently, these RHNs can decay and produce a lepton asymmetry while the washout processes are suppressed.

DOI: [10.1103/PhysRevD.106.035019](https://doi.org/10.1103/PhysRevD.106.035019)

I. INTRODUCTION

Baryogenesis via leptogenesis is an unavoidable consequence of $SO(10)$ grand unified theories (GUTs), which predict the existence of very heavy right-handed neutrinos (RHN), N , with mass-scale $M_N \gtrsim 10^{10}$ GeV [1,2]. While direct production of such heavy RHNs is not feasible in current or foreseeable future experiments, one can have indirect hints that high-scale leptogenesis occurred in nature. For instance, a particular $SO(10)$ symmetry breaking chain can be correlated with the proton lifetime and its associated gravitational wave (GW) signatures [3]. In principle, the observation/nonobservation of such as terrestrial and cosmological observables could constrain the RHN mass scale. Moreover, another interesting feature of $SO(10)$ GUTs is that leptogenesis is intimately connected with the Standard Model (SM) fermion masses [2], since each generation of fermions is unified within the same multiplet at the high scale. Nonetheless, in standard

cosmology, thermal leptogenesis is constrained from above by the perturbativity of the Yukawa couplings and by $\Delta L = 2$ scatterings, which can erase the lepton asymmetry. The strength of such washout processes increases with the temperature and the absolute light neutrino mass scale, m_ν . As the absolute mass scale may be measured in the near future, the focus of our paper is the correlation of m_ν with high-scale leptogenesis and how this parameter space may be enlarged due to the presence of primordial black holes (PBH).

The connection between m_ν and type-I thermal leptogenesis can be understood as follows. The leading CP -violating interactions of leptogenesis arise from the interference between tree-level and one-loop decay diagrams of $N \rightarrow \ell H$. This interference is schematically shown in Fig. 1 where the dashed orange line denotes the contribution when the leptonic and Higgs doublets (ℓ and H , respectively) go on their mass shells. The green square highlights the operator that violates lepton number by two units and contributes to the neutrino mass, m_ν , and the lepton-number-violating scattering amplitude e.g., $\bar{\ell} H^\dagger \leftrightarrow \ell H$ and $\ell \ell \leftrightarrow H^\dagger H^\dagger$. The red dot represents heavier degrees of freedom at a scale $\Lambda > M_N$ such as heavier generations of N and/or heavy Higgs $SU(2)_L$ triplet. Schematically, we can write the dimensionless CP violation parameter, ϵ , as

$$\frac{\epsilon}{M_N} \propto \frac{m_\nu}{v^2} \propto \sqrt{\sigma_{\Delta L=2}}, \quad (1.1)$$

*nicolas.bernal@uan.edu.co

†sheng.fong@ufabc.edu.br

‡yuber.f.perez-gonzalez@durham.ac.uk

§jessica.turner@durham.ac.uk

Published by the American Physical Society under the terms of the [Creative Commons Attribution 4.0 International license](https://creativecommons.org/licenses/by/4.0/). Further distribution of this work must maintain attribution to the author(s) and the published article's title, journal citation, and DOI. Funded by SCOAP³.

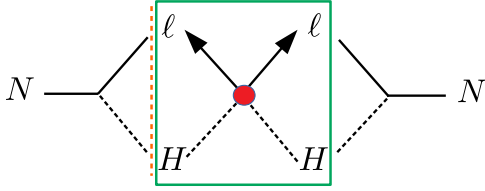


FIG. 1. The leading CP violation comes from the interference between the tree-level and one-loop level decay diagrams of $N \rightarrow \ell H$. The orange dashed line denotes the contribution when the loop particles go on their mass shell. The green square highlights the contribution to light neutrino mass as well as $\Delta L = 2$ scattering process for high-scale thermal leptogenesis.

where $v \simeq 174$ GeV is the SM Higgs vacuum expectation value and $\sigma_{\Delta L=2}$ is the cross section for scattering processes which violate lepton number by two units. In the above relation, we have assumed that the main contribution to the neutrino mass comes from the operator in the green square of Fig. 1, and we have estimated the cross-section in the regime $T \ll \Lambda$, with T the temperature of the SM thermal bath. The first relation in Eq. (1.1) leads to an upper limit on ϵ which depends on m_ν and M_N and is known as the Davidson-Ibarra bound [4].¹ Imposing a sufficiently large CP -violating parameter, $|\epsilon| \gtrsim 10^{-6}$, implies a lower bound on $M_N \gtrsim (0.1 \text{ eV}/m_\nu) \times 10^{10}$ GeV where we have included a one loop factor of $1/(16\pi)$ when relating ϵ to m_ν .

The $\Delta L = 2$ scattering processes in Eq. (1.1) become important when their rate exceeds the expansion rate of the Universe

$$\sigma_{\Delta L=2} \frac{T^3}{\pi^2} \sim \frac{m_\nu^2}{\pi^3 v^4} T^3 > H(T) \simeq 1.66 \sqrt{g_\star} \frac{T^2}{M_P}, \quad (1.2)$$

where we have included a phase space factor of $1/\pi$ for $\sigma_{\Delta L=2}$, and $H(T)$ corresponds to the Hubble expansion rate in a radiation dominated Universe with effective relativistic degrees of freedom g_\star , and the Planck mass is $M_P \simeq 1.22 \times 10^{19}$ GeV. This condition translates to $T \gtrsim 4(0.1 \text{ eV}/m_\nu)^2 \times 10^{12}$ GeV for $g_\star = 106.75$. While this relation is valid only up to $T \sim \Lambda$, it allows us to estimate when $\Delta L = 2$ scattering processes become relevant. Thermal leptogenesis suffers from strong washout from $\Delta L = 2$ scattering processes for $M_N \sim T \gtrsim 4(0.1 \text{ eV}/m_\nu)^2 \times 10^{12}$ GeV which will lead to upper bounds on both M_N and m_ν . The upper bound $m_\nu \lesssim 0.1$ eV has been derived previously such that $\Delta L = 2$ processes do not suppress the generated asymmetry [5,6]. While cosmological bounds give approximately the same

¹A careful derivation in Ref. [4] for type-I seesaw with hierarchical spectrum of N obtained ϵ which is bounded from above by $m_h - m_l$ with $m_h(m_l)$ is the heaviest (lightest) light neutrino mass.

bound [7], nonstandard cosmology [8] can still allow for large $m_\nu \sim \mathcal{O}(1)$ eV [9].

A possible way to evade the strong washout from $\Delta L = 2$ scatterings consists of generating a population of RHNs after those processes have frozen out. Moreover, some additional, nonthermal physical processes should intervene in the RHN production since the Yukawa interactions control both the RHN generation and washout in the standard scenario. A minimal framework that bypasses the requirement of additional degrees of freedom and/or interactions is particle production via Hawking radiation of PBHs [10].

Baryogenesis via PBH evaporation has attracted substantial attention since the discovery that BHs produce particles with a thermal spectrum [11–20]. Moreover, recent works have also considered the effects of evaporation in leptogenesis [21–24]. The interplay between thermal and PBH-assisted leptogenesis was discussed in detail in Ref. [21]. This work demonstrated that the PBH-produced RHNs can decay and produce a lepton asymmetry but that the entropy injection from the PBHs can dilute the lepton asymmetry, generated both nonthermally from the PBHs and thermally from the plasma, as PBHs are much more efficient at producing photons rather than RHNs. This dilutionary effect is most severe if the PBHs' mass exceeds $\sim \mathcal{O}(10^3)$ g. In this scenario, the baryon asymmetry obtained in the intermediate-scale thermal leptogenesis scenario (with the lightest RHN masses $10^6 \lesssim M_{N_1}(\text{GeV}) \lesssim 10^8$) would be diluted even in the most finely tuned regions of the parameter space.

In this work, we first explore generic baryogenesis where heavy particles X produced purely from PBH evaporation with their subsequent $B - L$ -violating and CP -violating decays, which generate a cosmic baryon asymmetry. Then, we study how light PBHs with masses smaller than $\mathcal{O}(1)$ g allow the evasion of the bound of $m_\nu \lesssim 0.1$ eV and open up the parameter space of very high-scale leptogenesis up to the GUT scale. The basic idea is that this population of light PBHs can evaporate at sufficiently high temperatures to produce a non-negligible abundance of RHNs when the ambient temperature of the SM plasma is sufficiently low such that the $\Delta L = 2$ scatterings are out of thermal equilibrium. Hence, the rapid decays of these PBH-produced RHNs generate a $B - L$ asymmetry when the washout processes are suppressed.² As a result, the upper bound on m_ν , which arises due to these scatterings, can be evaded. The direct/terrestrial measurement of the upper bound on the heaviest active neutrino mass comes from the endpoint measurement in the beta-decay spectrum and is around 0.8 eV [27]. If subsequent measurements determine

²It is interesting to note that particles (and in particular RHNs) heavier than the reheating temperature could still be produced in the early Universe during the reheating era if their mass is smaller than the highest temperature T_{max} reached by the thermal bath [25]. This corresponds to another viable scenario for leptogenesis [26].

neutrino masses to be large ($\gtrsim 0.1$ eV) then much of the parameter space of standard high-scale thermal leptogenesis would be excluded. However, if light PBHs once existed as a sizable fraction of the early Universe's energy budget, high-scale leptogenesis can still be a viable explanation for the observed matter-antimatter asymmetry.

The paper is organized as follows: in Sec. II we begin with a general discussion of PBH formation and evaporation as well as considering a generic PBH-assisted baryogenesis scenario. In Sec. III we summarize the relevant features of high-scale thermal leptogenesis and $\Delta L = 2$ washout processes and present the Boltzmann equations we numerically solve to study the interplay between very high-scale thermal leptogenesis and light PBHs. The main results of the paper are provided in Sec. IV, and we summarize and conclude in Sec. V. We use natural units in which $\hbar = c = k_B = 1$ throughout this manuscript.

II. BARYOGENESIS AND PRIMORDIAL BLACK HOLES

A. PBH formation and evaporation in a nutshell

PBHs could have been generated due to large density perturbations in the early Universe [10,28] and when these density fluctuations reenter the horizon, they can collapse to form a BH if they exceed a threshold [29]. This paper focuses on the case where PBHs form in a radiation-dominated epoch at an initial SM radiation temperature $T = T_0$. The initial PBH mass is related to the mass within the particle horizon as [30,31]

$$M_{\text{BH0}} = \frac{4\pi}{3} \alpha \frac{\rho_R(T_0)}{H^3(T_0)}, \quad (2.1)$$

where the gravitational collapse factor is $\alpha \sim 0.2$ in a radiation-dominated era, ρ_R corresponds to the SM radiation energy density, while the Hubble rate is given by

$$H = \sqrt{\frac{8\pi}{3} \frac{\rho_R}{M_P^2}} = \sqrt{\frac{4\pi^3 g_\star}{45} \frac{T^2}{M_P}}. \quad (2.2)$$

Here and in the following, we assume that the effective relativistic degrees of freedom, g_\star , is that of the SM $g_\star = 106.75$ for a bath temperature much above the weak scale. From Eq. (2.1), we can solve for the cosmic temperature, T_0 , when a PBH of mass, M_{BH0} , is formed

$$\begin{aligned} T_0 &= \frac{1}{2} \left(\frac{5}{g_\star \pi^3} \right)^{\frac{1}{4}} \sqrt{\frac{3\alpha M_P^3}{M_{\text{BH0}}}} \\ &\simeq 4.27 \times 10^{15} \text{ GeV} \left(\frac{106.75}{g_\star} \right)^{\frac{1}{4}} \left(\frac{1 \text{ g}}{M_{\text{BH0}}} \right)^{\frac{1}{2}} \left(\frac{\alpha}{0.2} \right)^{\frac{1}{2}}. \end{aligned} \quad (2.3)$$

This implies that after inflation, the thermal bath temperature should reheat at least to T_0 to form such a PBH. A lower bound on the initial PBH mass can be set once the upper bound on the inflationary scale is considered. The limit reported by the Planck collaboration $H_I \leq 2.5 \times 10^{-5} M_P$ [32] implies that $M_{\text{BH0}} \gtrsim 10^{-1}$ g. Since for gram-scale PBHs, the inflationary scale must be rather large, one may wonder if there are known mechanisms for formation of such light BHs. One such example can be found in Ref. [33] where they considered a scenario that leads to PBH masses below 10^6 g for some specific features of the Higgs potential. Thus, there could exist models that could predict the formation of very light PBHs. However, we remain agnostic regarding the formation mechanism in what follows. We define the initial PBH energy density over the radiation energy density as

$$\beta \equiv \frac{\rho_{\text{BH}}(T_0)}{\rho_R(T_0)} = \frac{n_0 M_{\text{BH0}}}{\rho_R(T_0)}, \quad (2.4)$$

where n_0 is the initial number density of PBHs, which we assume all have the same mass, M_{BH0} .³ Depending on the number density of PBHs generated in the early Universe, they could eventually dominate the energy density of the Universe, leading to a nonstandard cosmology [8].

After formation, the PBHs evaporate via the emission of all possible degrees of freedom in nature [10]. Throughout this work, we assume that PBHs are in the Schwarzschild phase and are therefore chargeless and spinless. The horizon radius, r_S , and the temperature for such a BH, T_{BH} , are given by

$$r_S = \frac{2M_{\text{BH}}}{M_P^2} \quad \text{and} \quad T_{\text{BH}} = \frac{M_P^2}{8\pi M_{\text{BH}}}, \quad (2.5)$$

respectively, with M_{BH} denoting the instantaneous BH mass. The rate of emission per energy interval of a particle of type i with mass m_i (in the limit $m_i \ll T_{\text{BH}}$) is given by

$$\frac{d^2 N_i}{dt dE} = \frac{g_i}{2\pi} \frac{\vartheta_i(M_{\text{BH}}, E)}{e^{E/T_{\text{BH}}} - (-1)^{2s_i}}, \quad (2.6)$$

where g_i and s_i denote the number of degrees of freedom and spin of particle i , respectively. The spin-dependent factor, $\vartheta_i(M_{\text{BH}}, E)$, in the Hawking emission rate, known as a graybody factor, describes the probability of a particle reaching spatial infinity. This graybody factor has an oscillatory behavior and tends toward the geometric optics limit $\vartheta_i(M_{\text{BH}}, E) \rightarrow 27r_S^2 E^2/4$ for large values of the energy E . From Eq. (2.6), the mass loss rate of a PBH can be determined as follows [36,37]

³In this work, we will not consider extended PBH mass functions that could arise if the PBHs are generated from inflationary density fluctuations or cosmological phase transitions, see, e.g., Refs. [34,35] for reviews.

$$\frac{dM_{\text{BH}}}{dt} = -\sum_i \int_{m_i}^{\infty} \frac{d^2 N_i}{dt dE} E dE = -\varepsilon(M_{\text{BH}}) \frac{M_P^4}{M_{\text{BH}}^2}, \quad (2.7)$$

where $\varepsilon(M_{\text{BH}})$ contains the information of the degrees of freedom that can be emitted during the evaporation process as a function of the instantaneous BH mass, see, e.g., Ref. [36,38].

Several bounds exist in the PBH parameter space spanned by the initial fraction β and mass M_{BH0} [31,35]. We will focus on PBHs that evaporated before big-bang nucleosynthesis (BBN), which have masses $\lesssim 10^9$ g. Although there exist constraints on such light PBHs, they are typically model dependent [31,35,39]. Nevertheless, recent constraints have been derived after considering the GWs emitted from the Hawking evaporation. In particular, a backreaction problem can be avoided if the energy contained in GWs never exceeds that of the background Universe [40]. More importantly, a modification of BBN predictions due to the energy density stored in GWs can be avoided if [41]

$$\beta \lesssim 1.1 \times 10^{-6} \left(\frac{\alpha}{0.2}\right)^{-\frac{1}{2}} \left(\frac{M_{\text{BH0}}}{10^4 \text{ g}}\right)^{-\frac{17}{24}}. \quad (2.8)$$

B. PBH-assisted baryogenesis

In this section, we consider a generic SM singlet particle X with mass, M_X , and internal degrees of freedom, g_X , that can decay and produce a $B - L$ asymmetry. We analytically estimate the number of X particles emitted by a PBH to determine the maximum baryon asymmetry that could be obtained from PBH evaporation only. We will omit the graybody factors and assume that the BH is a perfect black body, i.e., $\vartheta_i(M_{\text{BH}}, E) \rightarrow 1$. However, let us stress that we will include the graybody factors through our numerical treatment as detailed in Sec. III. As the emission of light or massless particles dominates the mass loss rate when $T_{\text{BH}} \gg m_i$, it is an excellent approximation to set $m_i = 0$, and hence we can obtain

$$\frac{dM_{\text{BH}}}{dt} \approx -\frac{g_* M_P^4}{30720\pi M_{\text{BH}}^2}. \quad (2.9)$$

For a PBH with initial mass M_{BH0} , its lifetime can be estimated as

$$\tau \approx -\int_{M_{\text{BH0}}}^0 \frac{30720\pi M_{\text{BH}}^2}{g_* M_P^4} dM_{\text{BH}} = \frac{10240\pi M_{\text{BH0}}^3}{g_* M_P^4}. \quad (2.10)$$

Assuming the Universe continues to be radiation dominated, we can compute the radiation temperature, T_{ev} , when the PBH population completely evaporates by setting the Hubble rate from Eq. (2.2) to be $H = 1/(2\tau)$, obtaining

$$\begin{aligned} T_{\text{ev}}|_{\text{Rad dom}} &\simeq \frac{1}{64} \left(\frac{g_*}{5\pi^5}\right)^{\frac{1}{4}} \sqrt{\frac{3M_P^5}{2M_{\text{BH0}}^3}} \\ &\simeq 1.22 \times 10^{10} \text{ GeV} \left(\frac{g_*}{106.75}\right)^{\frac{1}{4}} \left(\frac{1 \text{ g}}{M_{\text{BH0}}}\right)^{\frac{3}{2}}. \end{aligned} \quad (2.11)$$

On the other hand, if PBHs dominate the cosmic energy density before they completely evaporate, one should reevaluate the above estimation of T_{ev} as it will now depend on the initial abundance of the PBHs. Therefore, to determine T_{ev} , we have to solve for T_{ev} by setting $H = 2/(3\tau)$ and replacing the radiation energy density by the PBH energy density given in Eq. (2.2) and make the replacement $\rho_R \rightarrow \rho_M = M_{\text{BH0}} n(T_{\text{ev}})$ obtaining

$$\begin{aligned} T_{\text{ev}}|_{\text{PBH dom}} &\simeq \frac{1}{128} \left(\frac{g_* M_P^{10}}{10\pi^5 M_{\text{BH0}}^6 \beta T_0}\right)^{1/3} \\ &\simeq 4.11 \times 10^{10} \text{ GeV} \left(\frac{g_*}{106.75}\right)^{5/12} \\ &\quad \times \left(\frac{10^{-3}}{\beta}\right)^{1/3} \left(\frac{0.2}{\alpha}\right)^{1/6} \left(\frac{1 \text{ g}}{M_{\text{BH0}}}\right)^{11/6}. \end{aligned} \quad (2.12)$$

We emphasize that in the approximation where PBH instantaneously evaporate, T_{ev} corresponds to the SM temperature just before their sudden evaporation. The plasma temperature after evaporation could be found by taking into account the PBH entropy injection, and could be computed by the use of Eq. (2.17).

In principle, the X particles produced from the PBH evaporation could decay and produce the observed baryon asymmetry, depending on the Universe conditions when they were emitted. Let us assess the maximum amount of asymmetry that could be produced solely from the evaporation, neglecting the effects of the thermal plasma on such generation. The total number of X particles of mass M_X emitted over the lifetime of a PBH is given by

$$\begin{aligned} N_X &= \int_0^\tau dt \int_{M_X}^{\infty} dE \frac{d^2 N_X}{dt dE} \\ &= \int_{M_{\text{BH0}}}^0 dM_{\text{BH}} \frac{30720\pi M_{\text{BH}}^2}{g_* M_P^4} \int_{M_X}^{\infty} dE \frac{d^2 N_X}{dt dE}. \end{aligned} \quad (2.13)$$

One can solve the above equation in the two limits $M_X \ll T_{\text{BH0}}$ and $M_X \gg T_{\text{BH0}}$ where $T_{\text{BH0}} \equiv M_P^2/(8\pi M_{\text{BH0}})$ is the initial temperature of the PBH. Assuming that X is a fermion and matching the two solutions, we can approximate the total number of X emitted by a single PBH to be

$$N_X \simeq \frac{90\zeta(3)g_X}{\pi^3 g_\star} \times \begin{cases} \left(\frac{M_{\text{BH0}}}{M_P}\right)^2 & M_X \leq r_f T_{\text{BH0}}, \\ \frac{r_f^2}{64\pi^2} \left(\frac{M_P}{M_X}\right)^2 & M_X \geq r_f T_{\text{BH0}}, \end{cases} \quad (2.14)$$

where $r_f \equiv \sqrt{15\zeta(5)/\zeta(3)}$. Alternatively, the approximate solution if X is a boson is

$$N_X \simeq \frac{120\zeta(3)g_X}{\pi^3 g_\star} \times \begin{cases} \left(\frac{M_{\text{BH0}}}{M_P}\right)^2 & M_X \leq r_b T_{\text{BH0}}, \\ \frac{r_b^2}{64\pi^2} \left(\frac{M_P}{M_X}\right)^2 & M_X \geq r_b T_{\text{BH0}}, \end{cases} \quad (2.15)$$

where $r_b \equiv \sqrt{12\zeta(5)/\zeta(3)}$. The total number density of particle X produced from the evaporation of the PBHs normalized by cosmic entropy density, s , (before taking into account entropy injection from the evaporation of the PBHs) can be written as

$$Y_X^0 \equiv \frac{N_X n(T_{\text{ev}})}{s(T_{\text{ev}})} = \frac{N_X n_0}{s(T_0)} = \frac{3\beta T_0 N_X}{4M_{\text{BH0}}}, \quad (2.16)$$

where in the final equality, we have used the definition of Eq. (2.4) and $\rho_R(T_0)/s(T_0) = 3T_0/4$.

The entropy dilution from the complete evaporation of the PBHs can be estimated using conservation of energy before and after their evaporation⁴

$$\begin{aligned} \frac{\pi^2}{30} g_\star T_{\text{ev}}^4 + M_{\text{BH0}} \frac{n_0}{s(T_0)} s(T_{\text{ev}}) &= \frac{\pi^2}{30} g_\star \tilde{T}^4 \\ \Rightarrow \frac{s(\tilde{T})}{s(T_{\text{ev}})} &= \left(\frac{\tilde{T}}{T_{\text{ev}}}\right)^3 = \left(1 + \frac{\beta T_0}{T_{\text{ev}}}\right)^{3/4}, \end{aligned} \quad (2.17)$$

where \tilde{T} is the temperature of the SM plasma after PBH evaporation occurs.⁵ If the second factor in the bracket exceeds unity, then the PBHs come to dominate the energy density of the early Universe before they evaporate, resulting in entropy dilution after their complete evaporation. Here we emphasize that \tilde{T} is independent of β , even if PBHs eventually dominate the total energy density of the Universe. It was shown in e.g., Refs. [21,38,42–46] that the entropy injection from PBHs can affect the viable parameter space of baryogenesis and dark matter production, and therefore, such an effect cannot be neglected. Applying the dilution factor of Eq. (2.17) to Eq. (2.16), we find that the particle abundance after dilution is

⁴The additional entropy contribution from the decays of massive particle produced by PBHs with $T_{\text{BH0}} \sim m_i$ to the radiation will be suppressed by m_i/M_{BH0} and hence can be neglected.

⁵Alternatively, the entropy dilution can also be computed as in Ref. [42].

$$Y_X \equiv \frac{3\beta T_0 N_X s(T_{\text{ev}})}{4M_{\text{BH0}} s(\tilde{T})} = \frac{3\beta T_0 N_X}{4M_{\text{BH0}}} \left(1 + \beta \frac{T_0}{T_{\text{ev}}}\right)^{-3/4}. \quad (2.18)$$

Considering a fermionic X with $g_X = 2$, its final abundance from PBH evaporation is

$$Y_X \simeq \frac{135\zeta(3)}{\pi^3 g_\star} \beta \frac{T_0}{M_{\text{BH0}}} \left(1 + \beta \frac{T_0}{T_{\text{ev}}}\right)^{-3/4} \times \begin{cases} \left(\frac{M_{\text{BH0}}}{M_P}\right)^2 & M_X \leq r_f T_{\text{BH0}}, \\ \frac{15\zeta(5)}{64\pi^2 \zeta(3)} \left(\frac{M_P}{M_X}\right)^2 & M_X \geq r_f T_{\text{BH0}}. \end{cases} \quad (2.19)$$

In general, Eq. (2.19) can be applied since the entropy dilution term is relevant only when the PBHs dominate the cosmic energy density. Note that in the limit of large $\beta \frac{T_0}{T_{\text{ev}}} \gg 1$, the X abundance becomes independent of β . This can be understood as the compensation between the production of X and the entropy dilution from PBH evaporation, which also occurs in the case where X particles are produced from a hotter dark sector [47].

Assuming that the decays of X particles violate $B - L$ charge, the maximum baryon number asymmetry normalized by cosmic entropic density that can be obtained when X decays at $T \ll M_X$, but before the electroweak sphaleron freezes out, is given by [48]

$$Y_B^{\text{max}} = \frac{30}{97} Y_{B-L}^{\text{max}} = \frac{30}{97} \epsilon Y_X, \quad (2.20)$$

where ϵ is the CP violation parameter for the decay of X . For the conversion factor $30/97$, we have assumed that the electroweak sphaleron freezes out after electroweak symmetry breaking at $T \sim 130$ GeV as indicated by the lattice calculation [49] and excluded the top quark contribution [50]. The scenario above can occur if the X particles are long-lived and/or produced by PBH evaporation at $T \ll M_X$ when all washout processes are entirely suppressed. Equation (2.20) allows us to determine the minimum required $|\epsilon|$ by imposing such that Y_B^{max} is greater or equal to the observed value 8.7×10^{-11} [51] and this is plotted in Fig. 2 for several values of M_X . White regions are excluded as they correspond to $|\epsilon| \geq 1$. Taking $|\epsilon| = 1$ and requiring successful baryogenesis, we can estimate the upper bound on M_X using the second relation of Eq. (2.19) which gives

$$M_X \lesssim 1.3 \times 10^{17} \text{ GeV}, \quad (2.21)$$

where we have chosen $\beta = 10^{-3}$ and $M_{\text{BH0}} = 0.1$ g as reference values (in fact, we have saturated the upper bound on M_X for this large value of β). The parameter space for viable PBH-assisted baryogenesis increases with decreasing M_X because the production of X from PBH becomes more efficient despite the dilution from entropy production

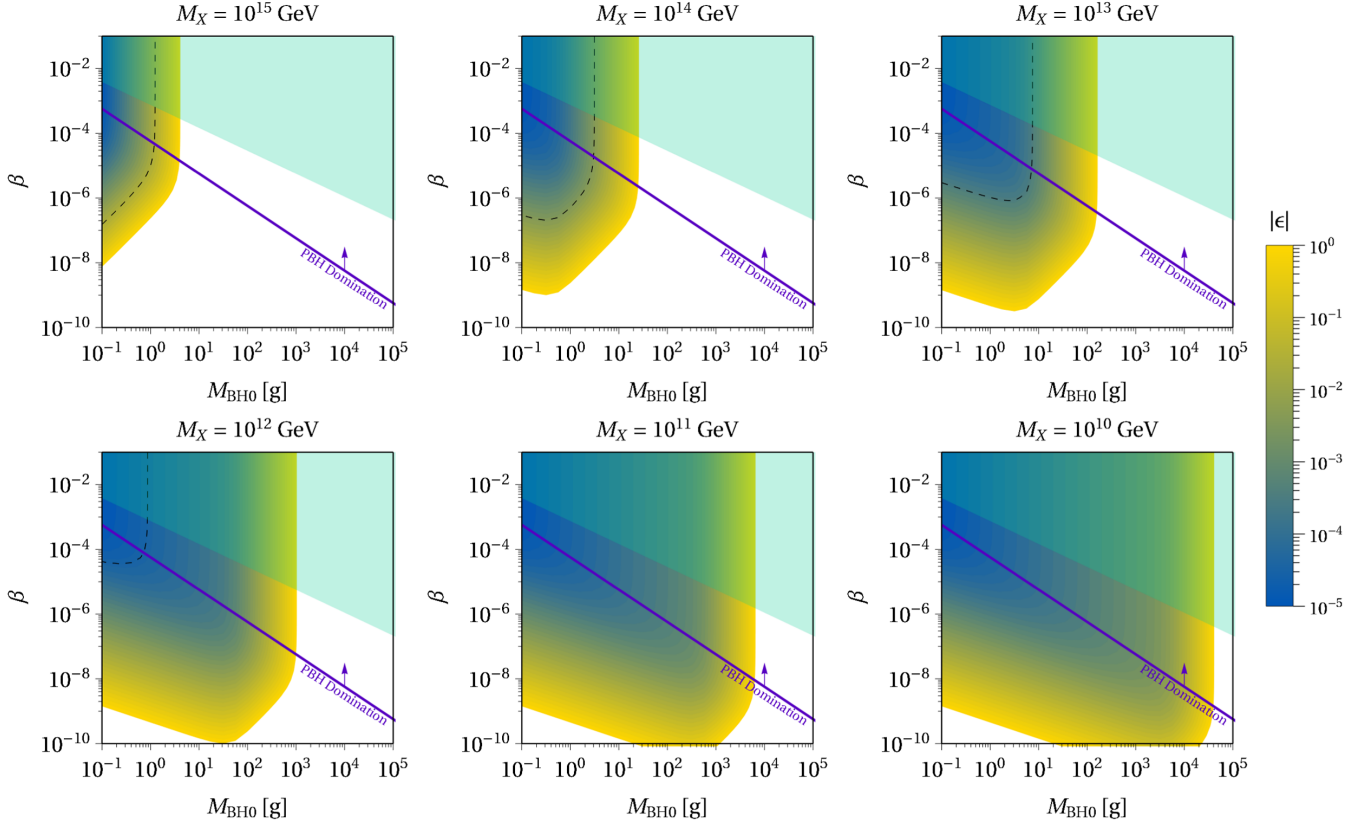


FIG. 2. Contours of CP violation parameter $|\epsilon|$ required for $M_X = 10^{15}, 10^{14}, 10^{13}, 10^{12}, 10^{11}$ and 10^{10} GeV (from left to right, top to bottom) taking into account the entropy production from PBH evaporation. The white regions are theoretically excluded while the dashed lines are the Davidson-Ibarra bound for the specific scenario of leptogenesis. For $M_{N_1} \lesssim 10^{12}$ GeV, we require tuning to achieve PBH leptogenesis. The green regions are excluded due GWs.

of PBHs. Considering the specific case of leptogenesis in the context of type-I seesaw mechanism with a hierarchical mass spectrum of RHNs, the Davidson-Ibarra bound on $|\epsilon|$ for leptogenesis from the lightest RHN, N_1 , with mass, M_{N_1} , is [4]

$$|\epsilon| \leq \frac{3M_{N_1}}{16\pi v^2} \frac{|\Delta m_{\text{atm}}^2|}{m_h + m_l}, \quad (2.22)$$

where $|\Delta m_{\text{atm}}^2| \equiv m_h^2 - m_l^2$ and $m_h(m_l)$ is the heaviest (lightest) light neutrino mass respectively. This limit is shown in Fig. 2 with dashed lines. Setting $|\Delta m_{\text{atm}}^2| = m_h^2 = (0.05 \text{ eV})^2 \gg m_l^2$. For $M_{N_1} \lesssim 10^{12}$ GeV, purely PBH leptogenesis would require tuning to evade the bound of Eq. (2.22), e.g., requiring a quasidegenerate RHN mass spectrum. Finally, the green regions are in tension with the GW bound in Eq. (2.8).

III. LEPTOGENESIS AND PRIMORDIAL BLACK HOLES

A. High-scale Leptogenesis and $\Delta L = 2$ Processes

High-scale leptogenesis and $\Delta L = 2$ processes As alluded to in Sec. I, we are interested in high-scale type-I leptogenesis

with seesaw scale $M_N \gtrsim 10^{12}$ GeV where there is a sensitivity to the absolute scale of light neutrino mass. At such high scales, due to large neutrino Yukawa coupling, the CP violation required for viable leptogenesis is naturally large without requiring a quasidegenerate RHN mass spectrum to enhance the CP violation resonantly. Therefore, we will focus on a mildly hierarchical RHN mass spectrum $M_{N_1} < M_{N_2} < M_{N_3}$, which, together with the strong wash-out condition, implies that tracking the dynamics of N_1 is sufficient as the contributions from N_2 and N_3 are suppressed. We will also ignore the lepton flavor effects as we consider the high-scale scenario. The relevant terms of the type-I seesaw Lagrangian are

$$-\mathcal{L} \supset \frac{1}{2} M_{N_i} \bar{N}_i^c N_i + \bar{\ell}_\alpha H^* \lambda_{\alpha i} N_i + \text{H.c.}, \quad (3.1)$$

where we consider three RHNs N_i ($i = 1, 2, 3$), the SM leptonic, ℓ_α ($\alpha = e, \mu, \tau$), and Higgs doublet H where the antisymmetric $SU(2)_L$ contractions are implicit. The CP violation parameter for leptogenesis from N_1 decays is defined as:

$$\epsilon \equiv \frac{\Gamma(N_1 \rightarrow \ell H) - \Gamma(N_1 \rightarrow \bar{\ell} H^\dagger)}{\Gamma_{N_1}}, \quad (3.2)$$

where we have summed over the final lepton flavors and Γ_{N_1} is the total N_1 decay width given by

$$\Gamma_{N_1} = \frac{(\lambda^\dagger \lambda)_{11} M_{N_1}}{8\pi}. \quad (3.3)$$

At leading order, the light neutrino mass matrix is given by the seesaw formula

$$m_\nu = -v^2 \lambda M_N^{-1} \lambda^T, \quad (3.4)$$

where $M_N = \text{diag}(M_{N_1}, M_{N_2}, M_{N_3})$. We will denote the light neutrino masses obtained from this matrix to be m_1 , m_2 and m_3 where we identify the solar mass splitting as $\Delta m_{\text{sol}}^2 = m_2^2 - m_1^2$.

To provide a conservative estimate of the maximum allowed parameter, we must fix certain free parameters that maximize $|\epsilon|$. Since $\Delta m_{\text{sol}}^2 \ll |\Delta m_{\text{atm}}^2|$, we can approximate $m_1 = m_2$ and using the Casas-Ibarra parametrization [52] there is only a single relevant complex angle of the R -matrix, $R = R(z_{13})$ [53]. Defining $z_{13} \equiv x + iy$, where x and y are real, the CP parameter in the hierarchical limit of RHN mass spectrum $M_{N_1} \ll M_{N_2}, M_{N_3}$, is given by

$$|\epsilon| = \frac{3M_{N_1}}{16\pi v^2} \frac{|\Delta m_{\text{atm}}^2|}{m_h + m_l} \frac{|\sin(2x) \sinh(2y)|}{\cosh(2y) - f \cos(2x)}, \quad (3.5)$$

where $f \equiv (m_3 - m_1)/(m_3 + m_1)$. Note that in the denominator, $\cosh(2y) - f \cos(2x) > 0$ given that $|f| < 1$. In the hierarchical mass limit for light neutrinos, for normal mass ordering $m_3 \gg m_1$ or inverse mass ordering $m_1 \gg m_3$, we have $f \rightarrow +1$ or $f \rightarrow -1$ respectively, while in the degenerate mass limit $m_3 \sim m_1$, we have $f \ll 1$. The maximum $|\epsilon|$ is given by $x = \pm\pi/4$ and $y \rightarrow \pm\infty$ which saturates to the Davidson-Ibarra bound of Eq. (2.22). However, as we will see in the following, a large y implies a large washout from inverse decays of N_1 . The degree of out-of-equilibrium decay of N_1 is quantified by the washout parameter defined as

$$K \equiv \frac{\Gamma_{N_1}}{H(T = M_{N_1})} \equiv \frac{\tilde{m}_1}{m_\star}, \quad (3.6)$$

where $H(T = M_{N_1})$ is the Hubble rate in a radiation-dominated Universe evaluated at $T = M_{N_1}$. In the second definition, $m_\star = \frac{16\pi^2 v^2}{3M_P} \sqrt{\frac{g_\star \pi}{5}} \simeq 10^{-3}$ eV while the effective neutrino mass can be expressed as

$$\tilde{m}_1 \equiv \frac{(\lambda^\dagger \lambda)_{11} v^2}{M_{N_1}} = \frac{m_h + m_l}{2} [\cosh(2y) - f \cos(2x)]. \quad (3.7)$$

Since for the heaviest neutrino $m_h > \sqrt{|\Delta m_{\text{atm}}^2|} \simeq 0.05$ eV, as long as $|y| > 0.14$, we will always be in the strong washout regime, $K > 1$. To determine the upper bound on the neutrino mass scale, m_h , the relevant regime is $m_h \gg \sqrt{|\Delta m_{\text{atm}}^2|}$ which also implies $m_h + m_l \rightarrow 2m_h$ and $f \ll 1$ and therefore

$$|\epsilon| = \frac{3M_{N_1}}{32\pi v^2} \frac{|\Delta m_{\text{atm}}^2 \sin(2x) \tanh(2y)|}{m_h}, \quad (3.8)$$

$$\tilde{m}_1 = m_h \cosh(2y). \quad (3.9)$$

In this regime, $K > \sqrt{|\Delta m_{\text{atm}}^2|}/m_\star \simeq 50$ and hence leptogenesis occurs in the strong washout regime. The CP violation parameter $|\epsilon|$ is maximized for $|x| = \pi/4$ while y should be determined such that $|\epsilon|$ is as large as possible without being overwhelmed by the inverse decay washout controlled \tilde{m}_1 . In this regime, an excellent approximation is to maximize $|\epsilon|/\tilde{m}_1$ which gives $|y| = \frac{1}{2} \log(1 + \sqrt{2}) \simeq 0.44$.

In the strong washout regime, the washout processes from inverse decays go out of equilibrium at $T \ll M_{N_1}$ and the asymmetry that survives is produced from decays of N_1 below this temperature. Hence, to determine the upper bound on m_h , we can approximate the total $\Delta L = 2$ washout process with the following squared amplitude valid for $T \ll M_{N_1}$ [5]

$$|\mathcal{A}|^2 = \frac{12s}{v^4} \text{Tr}(m_\nu^\dagger m_\nu), \quad (3.10)$$

where s is the center-of-mass energy squared. The thermally-averaged reaction density for $\Delta L = 2$ processes, assuming Maxwell-Boltzmann statistics, is

$$\gamma = \frac{T}{64\pi^4} \int_0^\infty ds \sqrt{s} \mathcal{K}_1\left(\frac{\sqrt{s}}{T}\right) \hat{\sigma}(s), \quad (3.11)$$

where $\mathcal{K}_i(x)$ is the modified Bessel function of order i and

$$\hat{\sigma}(s) = \frac{1}{8\pi s} \int_{-s}^0 |\mathcal{A}|^2 dt = \frac{3s}{2\pi v^4} \text{Tr}(m_\nu^\dagger m_\nu). \quad (3.12)$$

After integrating over s , we have

$$\gamma = \frac{3T^6}{4\pi^5 v^4} \text{Tr}(m_\nu^\dagger m_\nu). \quad (3.13)$$

We note that the interaction above has no Boltzmann suppression even if $T \ll M_{N_1}$ since the $\Delta L = 2$ scatterings ($\bar{\ell} H^\dagger \leftrightarrow \ell H$ and $\ell \ell \leftrightarrow H^\dagger H^\dagger$) do not involve external N_1 . Comparing γ/n with $n = T^3/\pi^2$ to the Hubble rate, this process will come into thermal equilibrium at a temperature of

$$T \gtrsim \frac{4\pi^3 v^4 \times 1.66\sqrt{g_\star}}{3\text{Tr}(m_\nu^\dagger m_\nu)M_P}, \quad (3.14)$$

assuming a radiation-dominated Universe. It is worth noting that $\text{Tr}(m_\nu^\dagger m_\nu) = \sum_i m_i^2$ and if this value is $8.5 \times 10^{-3} \text{ eV}^2$ (the current Planck + BOSS bound [7]), then the $\Delta L = 2$ scatterings need to be taken into account when $T \gtrsim 6.2 \times 10^{12} \text{ GeV}$. Let us consider leptogenesis which occurs at $T \sim M_{N_1}$ in which $\Delta L = 2$ scatterings are relevant. As the $\Delta L = 2$ scatterings are proportional to m_h^2 , increasing m_h will increase the $\Delta L = 2$ scattering rate such that the lepton asymmetry is erased and leptogenesis is no longer viable. We will determine the upper bound on m_h resulting from the washout effect of $\Delta L = 2$ scatterings numerically in the next section, with and without assuming the existence of PBHs.

As we are interested in the $m_h - M_{N_1}$ parameter space for viable high-scale leptogenesis we can make an estimation of the upper bound on M_{N_1} (without the existence of PBHs): as M_{N_1} is increased, $|\epsilon|$ will also increase. The maximum will be reached before violating perturbativity when $\epsilon \sim \mathcal{O}(1)$. Considering this upper bound on ϵ and that the largest $B - L$ asymmetry that can be generated in the strong washout regime is $Y_{B-L} \sim 10^{-4}|\epsilon|$, we can estimate the upper bound on M_{N_1} by restricting the additional exponential washout from $\Delta L = 2$ scatterings to be

$$\exp\left[-\int_{z_B}^{\infty} dz \frac{\gamma}{zHn}\right] \lesssim 10^{-6}, \quad (3.15)$$

where $z \equiv M_{N_1}/T$, and $z_B = M_{N_1}/T_B$ with T_B the temperature when the inverse decay rate becomes slower than the Hubble rate. The above restriction is to ensure that after taking into account the additional suppression factor above, we can still generate $Y_{B-L} \gtrsim 10^{-10}$ in accordance with observation [51]. Considering the least restrictive case $m_h = 0.05 \text{ eV}$ and $z_B \approx 3$ [5], we obtain an upper bound $M_{N_1} \lesssim 10^{15} \text{ GeV}$.

B. Boltzmann equations

In this section, we present the Friedmann and Boltzmann equations that we numerically solve to derive the m_h bound including the possible contribution from PBHs. The Friedmann equations for the comoving radiation ($\rho_R \equiv a^4 \rho_R$) and PBHs ($\rho_{\text{BH}} \equiv a^3 \rho_{\text{BH}}$) energy densities are

$$aH \frac{d\rho_R}{da} = -\frac{\epsilon_{\text{SM}}(M_{\text{BH}})}{\epsilon(M_{\text{BH}})} \frac{d \ln M_{\text{BH}}}{dt} a \rho_{\text{BH}}, \quad (3.16a)$$

$$aH \frac{d\rho_{\text{BH}}}{da} = \frac{d \ln M_{\text{BH}}}{dt} \rho_{\text{BH}}, \quad (3.16b)$$

$$H^2 = \frac{8\pi}{3M_P^2} (\rho_{\text{BH}} a^{-3} + \rho_R a^{-4}), \quad (3.16c)$$

where a is the scale factor, H the Hubble rate, and $\epsilon_{\text{SM}}(M_{\text{BH}})$ contains only the SM contribution to the evaporation. Note that we evolve with respect to a instead of z , in contrast to standard leptogenesis treatments. This is due to the possibly significant entropy dilution present in the PBH scenario. For convenience, we also track the evolution of the SM thermal plasma temperature, T [39,54,55]

$$aH \frac{dT}{da} = -\frac{T}{\Delta} \left\{ H + \frac{\epsilon_{\text{SM}}(M_{\text{BH}})}{\epsilon(M_{\text{BH}})} \frac{d \ln M_{\text{BH}}}{dt} \frac{g_\star(T)}{g_{\star s}(T)} \frac{a \rho_{\text{BH}}}{4 \rho_R} \right\}, \quad (3.17)$$

where Δ takes into account the change on the effective number of entropic degrees of freedom $g_{\star s}(T)$ in Eq. (3.16)

$$\Delta \equiv 1 + \frac{T}{3g_{\star s}(T)} \frac{dg_{\star s}(T)}{dT}. \quad (3.18)$$

Together with this set of equations, we solve the following momentum-integrated Boltzmann equations for the comoving thermal ($\mathcal{N}_{N_1}^{\text{TH}}$) and nonthermal ($\mathcal{N}_{N_1}^{\text{BH}}$) RHN densities [21]

$$aH \frac{d\mathcal{N}_{N_1}^{\text{TH}}}{da} = -(\mathcal{N}_{N_1}^{\text{TH}} - \mathcal{N}_{N_1}^{\text{eq}}) \Gamma_{N_1}^T, \quad (3.19a)$$

$$aH \frac{d\mathcal{N}_{N_1}^{\text{BH}}}{da} = -\mathcal{N}_{N_1}^{\text{BH}} \Gamma_{N_1}^{\text{BH}} + \mathcal{N}_{\text{BH}} \Gamma_{\text{BH} \rightarrow N_1}, \quad (3.19b)$$

where $\Gamma_{N_1}^T$ and $\mathcal{N}_{N_1}^{\text{eq}}$ are the thermally averaged decay rate and the equilibrium comoving abundance of the RHNs, respectively. $\Gamma_{N_1}^{\text{BH}}$ in Eq. (3.19b) is the decay width corrected by an average inverse time dilatation factor

$$\Gamma_{N_1}^{\text{BH}} \equiv \left\langle \frac{M_{N_1}}{E_{N_1}} \right\rangle_{\text{BH}} \Gamma_{N_1}, \quad (3.20)$$

where Γ_{N_1} is the RHN decay width defined in Eq. (3.3). It is worth emphasizing that the thermal average is taken with respect to the PBH instantaneous spectrum since the RHN energies are distributed according to the Hawking rate, which resembles a thermal distribution. To address the generation of RHNs from the PBH density, we have included a source term in Eq. (3.19b) equal to the comoving PBH number density, $\mathcal{N}_{\text{BH}} \equiv \rho_{\text{BH}}/M_{\text{BH}}$, times $\Gamma_{\text{BH} \rightarrow N_1}$, the total RHN emission rate per BH

$$\Gamma_{\text{BH} \rightarrow N_1} = \int_{M_{N_1}}^{\infty} dE \frac{d^2 N_{N_1}}{dt dE}. \quad (3.21)$$

The equation for the $B - L$ asymmetry, \mathcal{N}_{B-L} , is given by

$$aH \frac{d\mathcal{N}_{B-L}}{da} = \epsilon [(\mathcal{N}_{N_1}^{\text{TH}} - \mathcal{N}_{N_1}^{\text{eq}})\Gamma_{N_1}^T + \mathcal{N}_{N_1}^{\text{BH}}\Gamma_{N_1}^{\text{BH}}] + \left(\frac{1}{2}\Gamma_{N_1}^T \mathcal{N}_{N_1}^{\text{eq}} + \gamma \right) \frac{\mathcal{N}_{B-L}}{\mathcal{N}_\ell^{\text{eq}}}, \quad (3.22)$$

where ϵ is the CP parameter of Eq. (3.2) describing the decay asymmetry generated by N_1 , and $\mathcal{N}_\ell^{\text{eq}}$ is the lepton equilibrium abundance. The term proportional to \mathcal{N}_{B-L} corresponds to the washout processes including the $\Delta L = 2$ interactions discussed in Sec. III A. We compute the baryonic yield from the solution of the Friedmann-Boltzmann equations using

$$Y_B = \frac{30}{97} \frac{\mathcal{N}_{B-L}}{a_{\text{fn}}^3 s(T_{\text{fn}})}, \quad (3.23)$$

with a_{fn} and $s(T_{\text{fn}})$ are the scale factor and entropy density where we stop the evolution of the Boltzmann and Friedmann equations.

We solve the system of equations Eqs. (3.16), (3.19) and (3.22), together with the PBH mass rate, Eq. (2.7), to obtain the final baryon asymmetry. We make use of ULYSSES [56] which not only contains the infrastructure to solve equations for leptogenesis, but also has a library with the BH characteristics for the Schwarzschild and Kerr cases, and fitted forms of the total Hawking emission rate $\Gamma_{\text{BH} \rightarrow N_1}$. The code used in this work has been made publicly available within ULYSSES.⁶

IV. RESULTS AND DISCUSSION

As we are interested in obtaining the upper bound on the heaviest active neutrino mass m_h , we restrict ourselves to the strong washout regime. In this regime, we fix $|x| = \pi/4$ and $|y| = 0.44$, as detailed in Section III A, and consider a mild hierarchy of the RHN mass spectrum with $M_{N_3} > M_{N_2} > M_{N_1}$. We have verified that as long as the RHN mass spectrum is not quasi-degenerate, the upper bound on m_h is not sensitive to the specific hierarchy of M_{N_i} chosen. The main reason is that the upper bound is determined by $\Delta L = 2$ scatterings, which depend only on m_h and the temperature at which leptogenesis occurs. Since the upper bound on m_h is not very sensitive to the mass hierarchy of N 's, we will fix $M_{N_3} = 2M_{N_2} = 6M_{N_1}$ where it is a sufficiently good approximation to consider only N_1 -leptogenesis.

In the left panel of Fig. 3, the colored area on the left of the gray dotted line shows the successful parameter space i.e., $|Y_B| \geq Y_B^{\text{obs}}$ in the plane of m_h versus M_{N_1} for this standard scenario regime (i.e., no PBHs). We observe that

the upper bounds of $M_{N_1} \sim 10^{15}$ GeV and $m_h \sim 0.1$ eV are due to the sizable $\Delta L = 2$ washout as discussed in Sec. III A which are in agreement with Ref. [6]. The lower bound on M_{N_1} becomes more stringent with increasing m_h due to the Davidson-Ibarra bound, cf. Eq. (2.22). The purple hatched region corresponds to the current KATRIN bound, while the vertical dashed line is their projected future sensitivity [27] to the heaviest active neutrino mass, m_h . Next, we consider the additional effect of light PBHs on the m_h and seesaw scale parameter space. In the left panel of Fig. 3, we also overlay the successful parameter space for PBH-assisted scenario with $\beta = 10^{-4}$, and different PBHs masses: $M_{\text{BH}0} = 0.1$ g (solid red), 1 g (dashed blue), and 10 g (dash-dotted green). For $M_{\text{BH}0} = 0.1$ g, we observe that the viable parameter space is significantly enlarged such that even $m_h \sim 0.5$ eV and $M_{N_1} \sim 10^{16}$ GeV provides successful leptogenesis.

In fact, the upper bound on M_{N_1} can go beyond GUT scale up to Eq. (2.21) where N_1 particles are too heavy to be efficiently produced by PBH evaporation. For $M_{\text{BH}0} = 1$ g, the viable parameter space is smaller than for $M_{\text{BH}0} = 0.1$ g because the heavier the PBHs, the lower their initial temperature and therefore the less efficient they are at producing heavy RHNs via Hawking evaporation. Nonetheless, even PBHs with a gram-scale mass can significantly enlarge the viable parameter space. Finally, we observe that for $M_{\text{BH}0} = 10$ g, shown in green around $M_{N_1} \sim 10^{12}$ GeV, the viable parameter space shrinks compared to the PBH-less leptogenesis scenario. This occurs because the heavier PBHs are less efficient at producing such massive RHNs but they still provide sizable entropy injections into the early Universe plasma, diluting the baryon asymmetry produced from thermal leptogenesis. This tension between $\gtrsim \mathcal{O}(10)$ g PBHs and thermal leptogenesis has been discussed in detail in Ref. [21]. Interestingly, the successful region in this case presents a reduction around $M_{N_1} \sim 1.5 \times 10^{13}$ GeV and $m_h \sim 0.55$ eV. Such reduction appears because the entropy injection depletes the asymmetry produced thermally, while the RHNs produced from the evaporation are not sufficient to generate the observed baryon yield. On the other hand, for $M_{N_1} \lesssim 1.5 \times 10^{13}$ GeV, the PBHs emit efficiently RHNs which mitigate the dilution. For $M_{N_1} \gtrsim 1.5 \times 10^{13}$ GeV, the reduction due to the entropy from the evaporation is not strong enough to diminish the baryon asymmetry below the observed value.

Even though we expect that washout process to be switched off in the thermal SM bath, the particles produced during the evaporation should, in principle, heat up the plasma around the PBHs [57]. Thus, $\Delta L = 2$ processes might be active in the PBH vicinity, generating a washout of the final asymmetry. Although a complete determination of the washout in the PBH proximity lies beyond the scope of this paper, we can estimate whether the RH neutrino is able to escape the PBH before decaying. Considering all $2 \rightarrow 2$ processes for N_1 scattering [58], and taking the

⁶<https://github.com/earlyuniverse/ulysses>.

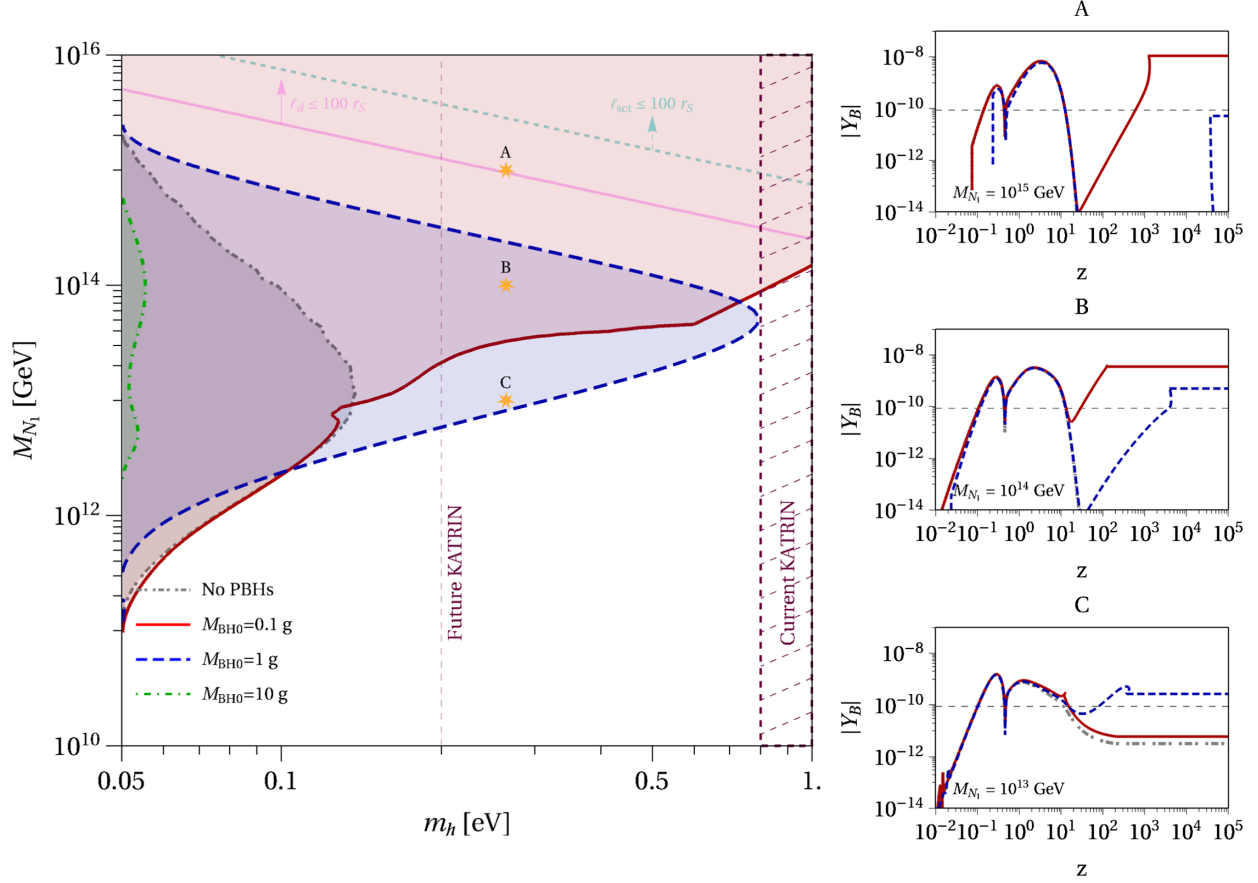


FIG. 3. Left: allowed parameter space for leptogenesis in the RH neutrino mass M_{N_1} vs heaviest active neutrino m_h plane for the standard scenario, i.e., no PBHs (gray dotted region) and including the contribution from evaporating PBHs having initial masses of $M_{\text{BH}0} = 0.1$ g (red region), $M_{\text{BH}0} = 1$ g (blue dashed region), $M_{\text{BH}0} = 10$ g (green dot-dashed region), while fixing $\beta = 10^{-4}$. The dashed region indicates the current KATRIN bound on m_h , while the dashed vertical line corresponds to their projected future sensitivity [27]. The magenta and cyan lines indicate the region where the N_1 decay length ℓ_d and mean free path ℓ_s are smaller than 100 times the Schwarzschild radius r_s , respectively. For such values, we could expect additional washout due to $\Delta L = 2$ processes that might be active around the PBH, see text. Right: evolution of the baryon yield $|Y_B|$ as function of $z = M_{N_1}/T$ for three different values of the RHN masses—indicated in the left panel by the stars— $M_{N_1} = 10^{15}$ GeV (top), $M_{N_1} = 10^{14}$ GeV (middle), $M_{N_1} = 10^{13}$ GeV (bottom), and $m_h = 0.27$ eV. The color indicates the different evolution in the presence of a PBH density with masses $M_{\text{BH}0} = 0.1$ g (red), $M_{\text{BH}0} = 1$ g (blue dashed), and in the standard case without PBHs (gray dotted).

plasma temperature to be the Hawking temperature, we can estimate the N_1 mean free path as

$$\begin{aligned} \ell_s &= \frac{4\pi}{\langle \tilde{\gamma}_N^{(0)} \rangle} \frac{v^2}{\tilde{m}_1 M_{N_1}} r_s \\ &\simeq 1.5 \times 10^3 r_s \left(\frac{0.5 \text{ eV}}{m_h} \right) \left(\frac{10^{14} \text{ GeV}}{M_{N_1}} \right), \end{aligned} \quad (4.1)$$

where $\langle \tilde{\gamma}_N^{(0)} \rangle \equiv \langle \gamma_N^{(0)} \rangle / T$, $\langle \gamma_N^{(0)} \rangle$ being the momentum-averaged N_1 scattering rate for vanishing leptonic chemical potential, taken from Ref. [58]. Similarly, the decay length is

$$\begin{aligned} \ell_d &= 8\pi \langle c \rangle \frac{v^2}{\tilde{m}_1 M_{N_1}^3} T = \begin{cases} \frac{\langle c \rangle}{2} \frac{v^2}{\tilde{m}_1 M_{N_1}^3} \frac{M_p^4}{M_{\text{BH}0}^2} r_s & \text{for } T_{\text{BH}0} \geq M_{N_1} \\ 16\pi^2 \langle c \rangle \frac{v^2}{\tilde{m}_1 M_{N_1}} r_s & \text{for } T_{\text{BH}0} < M_{N_1} \end{cases}, \\ &\simeq \begin{cases} 10 r_s \left(\frac{0.5 \text{ eV}}{m_h} \right) \left(\frac{10^{14} \text{ GeV}}{M_{N_1}} \right)^3 \left(\frac{1 \text{ g}}{M_{\text{BH}0}} \right)^2 & \text{for } T_{\text{BH}0} \geq M_{N_1} \\ 500 r_s \left(\frac{0.5 \text{ eV}}{m_h} \right) \left(\frac{10^{14} \text{ GeV}}{M_{N_1}} \right) & \text{for } T_{\text{BH}0} < M_{N_1} \end{cases}, \end{aligned} \quad (4.2)$$

where

$$\langle c \rangle = \left\langle \frac{M_{N_1}}{E} \right\rangle_{\text{BH}}^{-1} \frac{T_{\text{BH}}}{M_{N_1}} \simeq 3.72 \quad (4.3)$$

and $\langle M_{N_1}/E \rangle_{\text{BH}}$ is the thermally averaged time dilation factor for the N_1 decay, whose value has been determined numerically considering the full Hawking emission spectrum [21]. The previous estimations assume that the N_1 are produced at the horizon, even though the localization of the emitted particle at emission is meaningless since its Compton wavelength is of the same order as the Schwarzschild horizon. Thus, in a sense, our estimates are conservative. We present in Fig. 3 the region of the parameter space where $\ell_s \leq 100r_S$ and $\ell_d \leq 100r_S$, bounded by the cyan and magenta lines, respectively. For the decay length, we have that the relevant solution corresponds to the case where $T_{\text{BH}0} < M_{N_1}$. From this, we observe that the washout would affect mainly the asymmetry produced for $M_{\text{BH}0} = 0.1$ g, while we do not expect a significant modification for larger initial PBH masses. We leave a detailed discussion of the washout around a PBH for future work.

In the right panels of Fig. 3, we show the solutions to the Boltzmann and Friedmann equations for three points in the parameter space for fixed heaviest neutrino mass $m_h = 0.27$ eV and varying RHN masses: $M_{N_1} = 10^{15}$ GeV (point A), 10^{14} GeV (B) and 10^{13} GeV (C). For point A,

we observe that Y_B follows the thermal (gray dashed) solution until $z \sim 10$. At this point, light PBH evaporation starts to contribute effectively and produces RHNs which decay and generate a baryon asymmetry. The rapid change in gradient at $z \sim 10^3$ corresponds to the explosive evaporation that occurs at the end of the 0.1 g PBHs' lifetime. The same pattern is observed for PBHs of mass 1 g (dashed blue) but the evaporation is later, $z \sim 5 \times 10^4$, as the PBHs are heavier. Moreover, the final baryonic yield is lower since these heavier PBHs produce less RHNs. Finally, the purely thermal case (dashed gray) exhibits an exponential decrease in the baryonic yield at $z \sim 10$ due to the $\Delta L = 2$ washout being in thermal equilibrium. The behavior for point B is much the same as point A. For point C we observe that the evolution of the baryonic yield for the 0.1 g mass follows that of the thermal case, and it is the PBHs of mass 1 g that yield the larger baryon asymmetry. This occurs because the lighter PBHs, with 0.1 g mass, produce the RHNs with this lower mass scale earlier in their evolution when the $\Delta L = 2$ washout processes are still active. For $M_{\text{BH}0} = 10$ g the baryonic yield is so small that it is not shown on these plots.

In the left panel of Fig. 4, we plot Y_B with PBH-assisted leptogenesis normalized to the observed value Y_B^{obs} for a fixed $M_{N_1} = 10^{14}$ GeV. The more orange/yellow (green/blue) regions show an enhancement (depletion) of the

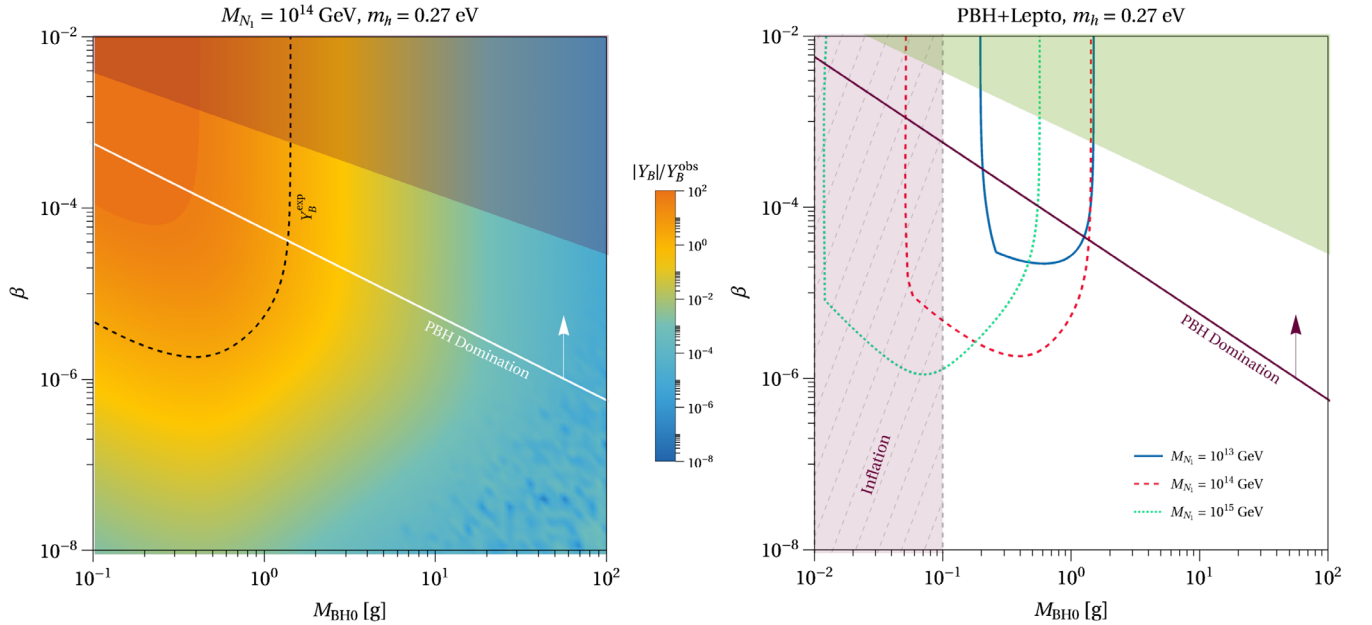


FIG. 4. Left: Y_B normalized to the observed value Y_B^{obs} for different values of the initial PBH density fraction β and mass $M_{\text{BH}0}$, taking $M_{N_1} = 10^{14}$ GeV and heaviest neutrino mass $m_h = 0.27$ eV. The dashed line corresponds to the region where we reproduce the measured baryon asymmetry. The white line indicates the PBH parameters which lead to a PBH-dominated era, and the darker region is in tension with GW observations. Right: initial PBH fraction β and mass $M_{\text{BH}0}$ parameters that generate the measured baryon yield for different values of the RHN masses, $M_{N_1} = 10^{13}$ GeV (blue), $M_{N_1} = 10^{14}$ GeV (red dashed), and $M_{N_1} = 10^{15}$ GeV (emerald dotted). The purple shaded region is excluded from inflation while the green region corresponds to the limit from GWs. The diagonal purple line indicates the parameters that lead to an early-PBH domination.

baryon asymmetry from PBHs. The area to the left of the dashed black line shows the region where the baryonic yield is equal to greater than the measured value. We observe that for this heavy RHN mass scale, gram or subgram scale PBHs ($\beta \gtrsim 10^{-6}$) are required for viable leptogenesis. Additionally, in the right panel of Fig. 4 we show the same range in β and $M_{\text{BH}0}$ for several masses of RHNs: $M_{N_1} = 10^{13}$ GeV (blue), 10^{14} GeV (red dashed), and 10^{15} GeV (emerald dotted), where the regions inside the colored lines are compatible with the observed baryonic yield. The purple (green) colored region is excluded by inflation (GWs). We note that the viable parameter space for larger N_1 masses shifts toward lighter PBH masses since the lighter PBHs are hotter initially and more efficient in producing heavier N_1 . The lower bound on the PBH mass is due to too early production of N_1 at the temperature when the $\Delta L = 2$ washout is still efficient while the upper bound on the PBH mass is due to the suppression of the production of N_1 because heavier PBHs are too cold to produce RHNs but still provide significant entropy production through their evaporation in the PBH domination regime. The viable parameter space shrinks for lower N_1 masses due to the Davidson-Ibarra bound in Eq. (2.22).

V. CONCLUSIONS

This work reevaluates viable high-scale thermal leptogenesis parameter space (in terms of the lightest RHN mass M_1 , and the heaviest active neutrino mass, m_h) in the presence of light PBHs. In the standard radiation dominated early Universe, if the lightest RHN mass exceeds $\sim 10^{15}$ GeV and heaviest active neutrino mass is greater than ~ 0.1 eV, $\Delta L = 2$ washout processes erase the lepton asymmetry. We have demonstrated that the presence of $\lesssim \mathcal{O}(1)$ g PBHs can provide a nonthermal source of RHNs produced via Hawking radiation when the SM plasma temperature is significantly lower than the lightest RHN mass. As such, the washout processes are ineffective, and a lepton asymmetry can be produced through the decays of these PBH sourced RHNs. While the leptogenesis parameter space is large, with 18 real parameters needed to determine the Yukawa matrix, we apply the Casas-Ibarra parametrization, assuming a mildly hierarchical RHN mass spectrum, fixing the leptonic mixing angles, mass squared splitting, and CP -violating phase at their best-fit values from global fit data [59] and fix the Majorana phases to be CP -conserving. The remaining parameters of the Yukawa matrix are fixed to maximize the lepton asymmetry without fine-tuning.

Applying these conservative assumptions, we numerically solve the relevant Friedmann and Boltzmann equations for PBH-assisted leptogenesis, and our main results can be found in Fig. 3, where the blue and red lines show the enlarged parameter space due to the light PBHs. Due to the presence of $\lesssim \mathcal{O}(1)$ g PBHs, we find that the upper bound on the lightest right-handed neutrino mass is generically given by $M_{N_1} \lesssim 10^{17}$ GeV up to consideration of the perturbativity of the Yukawa matrix or by $M_{N_1} \lesssim \text{few} \times 10^{15}$ GeV considering the possibility of heating of thermal bath in the vicinity of the PBHs. Furthermore, in this PBH-assisted leptogenesis scenario, the heaviest active neutrino mass, m_h , can be much larger 0.1 eV. Although this is in tension with the current cosmological bound $\sum_i m_i < 0.16$ eV [7], nonstandard cosmology could allow $m_h \sim 1$ eV [9]. The direct neutrino mass measurement from KATRIN gives $m_h < 0.8$ eV while the final sensitivity could go down to 0.2 eV [27], essentially probing all the new parameters allowed by PBH-assisted leptogenesis. To summarize, the expansion of the viable parameter space (in the $M_{N_1} - m_h$ plane) implies that high-scale leptogenesis, excluded in a standard cosmology if neutrino masses are measured to be large ($\gtrsim 0.1$ eV), could be rescued if gram-scale PBHs once constituted a sizable fraction of the energy density of the Universe.

ACKNOWLEDGMENTS

N. B. received funding from the Spanish FEDER/MCIU-AEI under grant No. FPA2017-84543-P, and the Patrimonio Autónomo—Fondo Nacional de Financiamiento para la Ciencia, la Tecnología y la Innovación Francisco José de Caldas (MinCiencias—Colombia) Grants No. 80740-465-2020 and No. 80740-492-2021. C. S. F. acknowledges the support by FAPESP Grant No. 2019/11197-6 for the project “Precision baryogenesis” and CNPq Grant No. 301271/2019-4. This work used the DiRAC@Durham facility managed by the Institute for Computational Cosmology on behalf of the STFC DiRAC HPC Facility [60]. The equipment was funded by BEIS capital funding via STFC capital Grants No. ST/P002293/1, No. ST/R002371/1, and No. ST/S002502/1, Durham University and STFC operations grant No. ST/R000832/1. DiRAC is part of the National e-Infrastructure. This work has also used the Hamilton HPC Service of Durham University. This project has received funding/support from the European Union’s Horizon 2020 research and innovation programme under the Marie Skłodowska-Curie Grant agreement No. 860881-HIDDeN.

- [1] P. Di Bari and A. Riotto, Successful type I leptogenesis with SO(10)-inspired mass relations, *Phys. Lett. B* **671**, 462 (2009).
- [2] C. S. Fong, D. Meloni, A. Meroni, and E. Nardi, Leptogenesis in SO(10), *J. High Energy Phys.* **01** (2015) 111.
- [3] S. F. King, S. Pascoli, J. Turner, and Y.-L. Zhou, Confronting SO(10) GUTs with proton decay and gravitational waves, *J. High Energy Phys.* **10** (2021) 225.
- [4] S. Davidson and A. Ibarra, A lower bound on the right-handed neutrino mass from leptogenesis, *Phys. Lett. B* **535**, 25 (2002).
- [5] W. Buchmuller, P. Di Bari, and M. Plumacher, Leptogenesis for pedestrians, *Ann. Phys. (Amsterdam)* **315**, 305 (2005).
- [6] G. F. Giudice, A. Notari, M. Raidal, A. Riotto, and A. Strumia, Towards a complete theory of thermal leptogenesis in the SM and MSSM, *Nucl. Phys.* **B685**, 89 (2004).
- [7] M. M. Ivanov, M. Simonović, and M. Zaldarriaga, Cosmological parameters and neutrino masses from the final planck and full-shape BOSS data, *Phys. Rev. D* **101**, 083504 (2020).
- [8] R. Allahverdi *et al.*, The first three seconds: A review of possible expansion histories of the early universe, *Open J. Astrophys.* **4** (2020).
- [9] J. Alvey, M. Escudero, N. Sabti, and T. Schwetz, Cosmic neutrino background detection in large-neutrino-mass cosmologies, *Phys. Rev. D* **105**, 063501 (2022).
- [10] S. W. Hawking, Particle creation by black holes, *Commun. Math. Phys.* **43**, 199 (1975).
- [11] D. Toussaint, S. B. Treiman, F. Wilczek, and A. Zee, Matter-antimatter accounting, thermodynamics, and black hole radiation, *Phys. Rev. D* **19**, 1036 (1979).
- [12] S. W. Hawking, Interacting quantum fields around a black hole, *Commun. Math. Phys.* **80**, 421 (1981).
- [13] J. D. Barrow, E. J. Copeland, E. W. Kolb, and A. R. Liddle, Baryogenesis in extended inflation. 2. Baryogenesis via primordial black holes, *Phys. Rev. D* **43**, 984 (1991).
- [14] A. S. Majumdar, P. Das Gupta, and R. P. Saxena, Baryogenesis from black hole evaporation, *Int. J. Mod. Phys. D* **04**, 517 (1995).
- [15] E. V. Bugaev, M. G. Elbakidze, and K. V. Konishchev, Baryon asymmetry of the universe from evaporation of primordial black holes, *Phys. At. Nucl.* **66**, 476 (2003).
- [16] D. Baumann, P. J. Steinhardt, and N. Turok, Primordial black hole baryogenesis, [arXiv:hep-th/0703250](https://arxiv.org/abs/hep-th/0703250).
- [17] T. Fujita, M. Kawasaki, K. Harigaya, and R. Matsuda, Baryon asymmetry, dark matter, and density perturbation from primordial black holes, *Phys. Rev. D* **89**, 103501 (2014).
- [18] L. Morrison, S. Profumo, and Y. Yu, Melanopogenesis: Dark matter of (almost) any mass and baryonic matter from the evaporation of primordial black holes weighing a ton (or less), *J. Cosmol. Astropart. Phys.* **05** (2019) 005.
- [19] A. Ambrosone, R. Calabrese, D. F. G. Fiorillo, G. Miele, and S. Morisi, Towards baryogenesis via absorption from primordial black holes, *Phys. Rev. D* **105**, 045001 (2022).
- [20] D. Hooper and G. Krnjaic, GUT baryogenesis with primordial black holes, *Phys. Rev. D* **103**, 043504 (2021).
- [21] Y. F. Perez-Gonzalez and J. Turner, Assessing the tension between a black hole dominated early universe and leptogenesis, *Phys. Rev. D* **104**, 103021 (2021).
- [22] S. Datta, A. Ghosal, and R. Samanta, Baryogenesis from ultralight primordial black holes and strong gravitational waves from cosmic strings, *J. Cosmol. Astropart. Phys.* **08** (2021) 021.
- [23] S. Jyoti Das, D. Mahanta, and D. Borah, Low scale leptogenesis and dark matter in the presence of primordial black holes, *J. Cosmol. Astropart. Phys.* **11** (2021) 019.
- [24] B. Barman, D. Borah, S. J. Das, and R. Roshan, Non-thermal origin of asymmetric dark matter from inflaton and primordial black holes, *J. Cosmol. Astropart. Phys.* **03** (2022) 031.
- [25] G. F. Giudice, E. W. Kolb, and A. Riotto, Largest temperature of the radiation era and its cosmological implications, *Phys. Rev. D* **64**, 023508 (2001).
- [26] N. Bernal and C. S. Fong, Dark matter and leptogenesis from gravitational production, *J. Cosmol. Astropart. Phys.* **06** (2021) 028.
- [27] KATRIN Collaboration, Direct neutrino-mass measurement with sub-electronvolt sensitivity, *Nat. Phys.* **18**, 160 (2022).
- [28] B. J. Carr and S. W. Hawking, Black holes in the early Universe, *Mon. Not. R. Astron. Soc.* **168**, 399 (1974).
- [29] W. H. Press and P. Schechter, Formation of galaxies and clusters of galaxies by self-similar gravitational condensation, *Astrophys. J.* **187**, 425 (1974).
- [30] B. J. Carr, K. Kohri, Y. Sendouda, and J. Yokoyama, New cosmological constraints on primordial black holes, *Phys. Rev. D* **81**, 104019 (2010).
- [31] B. Carr, K. Kohri, Y. Sendouda, and J. Yokoyama, Constraints on primordial black holes, *Rep. Prog. Phys.* **84**, 116902 (2021).
- [32] Planck Collaboration, Planck 2018 results. X. Constraints on inflation, *Astron. Astrophys.* **641**, A10 (2020).
- [33] S. Rasanen and E. Tomberg, Planck scale black hole dark matter from Higgs inflation, *J. Cosmol. Astropart. Phys.* **01** (2019) 038.
- [34] M. Sasaki, T. Suyama, T. Tanaka, and S. Yokoyama, Primordial black holes—perspectives in gravitational wave astronomy, *Classical Quantum Gravity* **35**, 063001 (2018).
- [35] B. Carr and F. Kuhnel, Primordial black holes as dark matter: Recent developments, *Annu. Rev. Nucl. Part. Sci.* **70**, 355 (2020).
- [36] J. H. MacGibbon and B. R. Webber, Quark and gluon jet emission from primordial black holes: The instantaneous spectra, *Phys. Rev. D* **41**, 3052 (1990).
- [37] J. H. MacGibbon, Quark and gluon jet emission from primordial black holes. 2. The lifetime emission, *Phys. Rev. D* **44**, 376 (1991).
- [38] A. Cheek, L. Heurtier, Y. F. Perez-Gonzalez, and J. Turner, Primordial black hole evaporation and dark matter production. I. Solely Hawking radiation, *Phys. Rev. D* **105**, 015022 (2022).
- [39] C. Lunardini and Y. F. Perez-Gonzalez, Dirac and Majorana neutrino signatures of primordial black holes, *J. Cosmol. Astropart. Phys.* **08** (2020) 014.
- [40] T. Papanikolaou, V. Vennin, and D. Langlois, Gravitational waves from a universe filled with primordial black holes, *J. Cosmol. Astropart. Phys.* **03** (2021) 053.
- [41] G. Domènech, C. Lin, and M. Sasaki, Gravitational wave constraints on the primordial black hole dominated early universe, *J. Cosmol. Astropart. Phys.* **04** (2021) 062.

- [42] N. Bernal, F. Hajkarim, and Y. Xu, Axion dark matter in the time of primordial black holes, *Phys. Rev. D* **104**, 075007 (2021).
- [43] N. Bernal and Ó. Zapata, Self-interacting dark matter from primordial black holes, *J. Cosmol. Astropart. Phys.* **03** (2021) 007.
- [44] N. Bernal and Ó. Zapata, Dark matter in the time of primordial black holes, *J. Cosmol. Astropart. Phys.* **03** (2021) 015.
- [45] A. Cheek, L. Heurtier, Y. F. Perez-Gonzalez, and J. Turner, Primordial black hole evaporation and dark matter production. II. Interplay with the freeze-in or freeze-out mechanism, *Phys. Rev. D* **105**, 015023 (2022).
- [46] N. Bernal, Y. F. Perez-Gonzalez, Y. Xu, and Ó. Zapata, ALP dark matter in a primordial black hole dominated Universe, *Phys. Rev. D* **104**, 123536 (2021).
- [47] N. Bernal and C. S. Fong, Hot leptogenesis from thermal dark matter, *J. Cosmol. Astropart. Phys.* **10** (2017) 042.
- [48] C. S. Fong, Baryogenesis in the Standard Model and its supersymmetric extension, *Phys. Rev. D* **103**, L051705 (2021).
- [49] M. D’Onofrio, K. Rummukainen, and A. Tranberg, Sphaleron Rate in the Minimal Standard Model, *Phys. Rev. Lett.* **113**, 141602 (2014).
- [50] T. Inui, T. Ichihara, Y. Mimura, and N. Sakai, Cosmological baryon asymmetry in supersymmetric Standard Models and heavy particle effects, *Phys. Lett. B* **325**, 392 (1994).
- [51] Planck Collaboration, Planck 2018 results. VI. Cosmological parameters, *Astron. Astrophys.* **641**, A6 (2020).
- [52] J. A. Casas and A. Ibarra, Oscillating neutrinos and $\mu \rightarrow e, \gamma$, *Nucl. Phys.* **B618**, 171 (2001).
- [53] T. Hambye, Y. Lin, A. Notari, M. Papucci, and A. Strumia, Constraints on neutrino masses from leptogenesis models, *Nucl. Phys.* **B695**, 169 (2004).
- [54] N. Bernal and F. Hajkarim, Primordial gravitational waves in nonstandard cosmologies, *Phys. Rev. D* **100**, 063502 (2019).
- [55] P. Arias, N. Bernal, A. Herrera, and C. Maldonado, Reconstructing non-standard cosmologies with dark matter, *J. Cosmol. Astropart. Phys.* **10** (2019) 047.
- [56] A. Granelli, K. Moffat, Y. F. Perez-Gonzalez, H. Schulz, and J. Turner, ULYSSES: Universal LeptogeneSiS equation solver, *Comput. Phys. Commun.* **262**, 107813 (2021).
- [57] S. Das and A. Hook, Black hole production of monopoles in the early universe, *J. High Energy Phys.* **12** (2021) 145.
- [58] P. Hernández, M. Kekic, J. López-Pavón, J. Racker, and J. Salvado, Testable baryogenesis in seesaw models, *J. High Energy Phys.* **08** (2016) 157.
- [59] I. Esteban, M. C. Gonzalez-Garcia, M. Maltoni, T. Schwetz, and A. Zhou, The fate of hints: Updated global analysis of three-flavor neutrino oscillations, *J. High Energy Phys.* **09** (2020) 178.
- [60] www.dirac.ac.uk.